

AIAA 81-0999AR

Generation of Boundary-Conforming Grids Around Wing-Body Configurations Using Transfinite Interpolation

L. E. Eriksson*

FFA The Aeronautical Research Institute of Sweden, Bromma, Sweden

A computational procedure for generating three-dimensional nonorthogonal surface-fitted mesh systems around wing-fuselage configurations is presented. The method is based on the concept of transfinite interpolation, which has been extended to handle very general mapping function specifications at the boundaries, thereby making it possible to generate single-block mappings with geometry data specified only at the outer boundaries of the computational domain. Since it is a direct algebraic mapping technique, the method is very inexpensive in terms of computer cost. Different types of possible mappings are compared with respect to resolution and economy of nodal points. A procedure for a novel type of mapping, designated type O-O, is described and several plots of generated grids demonstrate the capabilities of the method. The singular lines inherent in every three-dimensional mesh for this type of surface geometry are also discussed.

Introduction

THE construction itself of a coordinate mesh around even a simple wing-body configuration is not a trivial matter; and the numerical solution of the governing partial differential equations upon it is indeed a formidable computational task, which in turn puts a high premium on a mesh generator that can provide an optimum resolution with an economy of nodal points. It is felt that these two items, mesh construction and solution procedure, are separate and distinct operations, and as such should be treated in an independent and modular way, i.e., the means for generating a mesh should not be dictated by the limitations of a given specific flow-solution procedure and conversely the method that determines the flow should accept as input an arbitrary set of coordinate points which constitutes the mesh. In practice, of course, these two operations can never be totally independent because the logistic structure of the data, the location of outer boundaries, the nature of coordinate cuts, and the types of mesh singularities are items that have to be closely coordinated between the flow solver and the mesh generator.

The present method of constructing a three-dimensional boundary-conforming grid for a wing-body configuration is a direct algebraic approach based on the concept of transfinite or multivariate interpolation. A significant extension of the original formulation by Gordon and Hall¹ has made it possible to generate global single block transformations with geometry specifications only on the outer boundaries of the computational domain and yet obtain a high degree of local control. This generalized method² was presented at a workshop on grid generation at NASA Langley in 1980. Due to the generality of the method it has been possible to use more advanced mappings than conventional types and thereby improve the overall efficiency of the grid in terms of computational work for a given resolution. In this work, a qualitative analysis of several alternative types of mappings is presented and also the application of the generalized transfinite interpolation method to generate a novel type of mapping designated type O-O is described. An important subtopic in this context is the matter of singularities and this subject is discussed in some detail. It is believed that the general classification of different types of singularities and the way they are related to the type of mapping used is a

necessary first step in the long term process of understanding the effect of singularities on the computational results.

The generation of a reasonable grid for a wing or a wing-body configuration is, of course, only the first step of the overall flow computation task and the final proof that the generated grid is "good" or "bad" is the actual computational result. In Ref. 3, solutions to the Euler equations are presented, using a time-dependent finite-volume scheme and meshes of the O-O type generated by the present method. The results demonstrate that the grid generation procedure described here is capable of producing meshes suitable for these cases.

Transfinite Interpolation

The theory of transfinite interpolation as described by Gordon and Hall¹ is a very general concept of multivariate interpolation and is outlined briefly. Let $f(u, v, w) = [x(u, v, w), y(u, v, w), z(u, v, w)]$ denote a vector-valued function of three parameters u, v, w defined on the region $u_1 \leq u \leq u_p$, $v_1 \leq v \leq v_q$, $w_1 \leq w \leq w_r$. This function is not known throughout the region, only on certain planes (Fig. 1).

$$f(u_k, v, w) = a_k(v, w); \quad k = 1, 2, \dots, p$$

$$f(u, v_k, w) = b_k(u, w); \quad k = 1, 2, \dots, q$$

$$f(u, v, w_k) = c_k(u, v); \quad k = 1, 2, \dots, r$$

To interpolate between these given planes we need to define a set of univariate blending functions

$$\alpha_k(u); \quad k = 1, 2, \dots, p$$

$$\beta_k(v); \quad k = 1, 2, \dots, q$$

$$\gamma_k(w); \quad k = 1, 2, \dots, r$$

which only have to satisfy the conditions

$$\alpha_k(u_\ell) = \delta_{k\ell}; \quad \beta_k(v_\ell) = \delta_{k\ell}; \quad \gamma_k(w_\ell) = \delta_{k\ell}$$

where

$$\delta_{k\ell} = 0; \quad k \neq \ell \quad \delta_{k\ell} = 1; \quad k = \ell$$

Presented as part of Paper 81-0999 at the AIAA Fifth Computational Fluid Dynamics Conference, Palo Alto, Calif., June 22-23, 1981; submitted June 22, 1981; revision received Jan. 4, 1982. Copyright © 1982 by L. E. Eriksson. Published by the American Institute of Aeronautics and Astronautics, Inc., with permission.

*Research Scientist, Aerodynamics Department.

The transfinite interpolation procedure then gives the interpolated function $f(u, v, w)$ by the recursive algorithm

$$f_1(u, v, w) = \sum_{k=1}^p \alpha_k(u) a_k(v, w)$$

$$f_2(u, v, w) = f_1(u, v, w) + \sum_{k=1}^q \beta_k(v) [b_k(u, w) - f_1(u, v_k, w)]$$

$$f(u, v, w) = f_2(u, v, w) + \sum_{k=1}^r \gamma_k(w) [c_k(u, v) - f_2(u, v, w_k)] \tag{1}$$

The function f now defines a transformation from the region $u_1 \leq u \leq u_p, v_1 \leq v \leq v_q, w_1 \leq w \leq w_r$ in u, v, w space to some arbitrarily shaped region in the x, y, z space. In principle, each step of the algorithm consists of a univariate interpolation in one of the three possible directions (u, v , or w) and it is, of course, possible to reduce the three-step formula to only one single expression. It is then easy to verify that if the specification of f on the planes $u = u_1, \dots, u_p, v = v_1, \dots, v_q$, and $w = w_1, \dots, w_r$ is continuous at the intersections of these planes, the explicit order of the interpolation directions chosen in the three-step algorithm does not affect the interpolant.

For typical three-dimensional grid generation problems, there is a need to minimize the required input geometry data while retaining a high degree of control of the transformation, at least near the surfaces of interest. The interpolation procedure just described can give any degree of control if a sufficient number of internal surfaces are specified, but if no internal surface is defined at all (f is specified only on the outer surfaces of the parametric box), the control is generally poor. In order to improve the control in this case, a generalized transfinite interpolation procedure² which uses derivatives of the function f in the out-of-surface direction, in addition to the function itself, can be defined. The effect of specifying out-of-surface derivatives of f (Fig. 2) is to introduce a direct control of the essential properties of the mapping function in the vicinity of the surface. The specified data are then written

$$\frac{\partial^n}{\partial u^n} f(u_k, v, w) = a_k^{(n)}(v, w); \quad k=1,2 \quad n=0,1,2,\dots,p_k$$

$$\frac{\partial^n}{\partial v^n} f(u, v_k, w) = b_k^{(n)}(u, w); \quad k=1,2 \quad n=0,1,2,\dots,q_k$$

$$\frac{\partial^n}{\partial w^n} f(u, v, w_k) = c_k^{(n)}(u, v); \quad k=1,2 \quad n=0,1,2,\dots,r_k$$

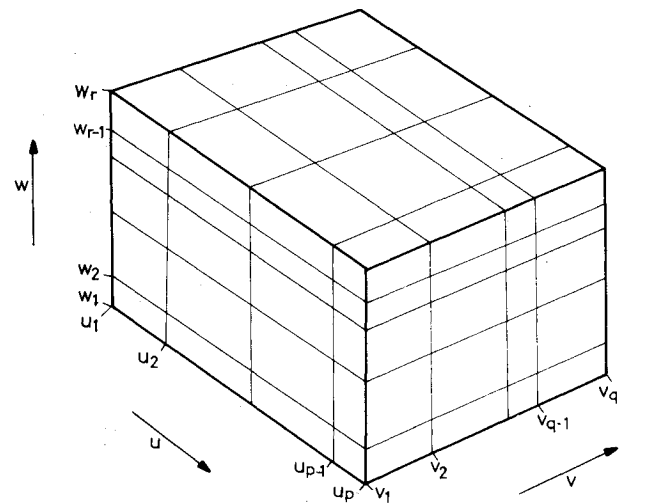


Fig. 1 The parametric domain with $f(u, v, w)$ specified on planes of constant u, v , or w .

which is simply the specification of f and a finite number of out-of-surface derivatives of f on the outer surfaces of the region $u_1 \leq u \leq u_2, v_1 \leq v \leq v_2, w_1 \leq w \leq w_2$ in u, v, w space (Fig. 3). To interpolate f into the interior of this parametric box, we define a new set of univariate blending functions

$$\alpha_k^{(n)}(u); \quad k=1,2 \quad n=0,1,2,\dots,p_k$$

$$\beta_k^{(n)}(v); \quad k=1,2 \quad n=0,1,2,\dots,q_k$$

$$\gamma_k^{(n)}(w); \quad k=1,2 \quad n=0,1,2,\dots,r_k$$

which only have to satisfy the conditions

$$\frac{\partial^m}{\partial u^m} \alpha_k^{(n)}(u_\ell) = \delta_{k\ell} \delta_{nm}; \quad \frac{\partial^m}{\partial v^m} \beta_k^{(n)}(v_\ell) = \delta_{k\ell} \delta_{nm}$$

$$\frac{\partial^m}{\partial w^m} \gamma_k^{(n)}(w_\ell) = \delta_{k\ell} \delta_{nm}$$

The generalized transfinite interpolation algorithm is then written

$$f_1(u, v, w) = \sum_{k=1}^2 \sum_{n=0}^{p_k} \alpha_k^{(n)}(u) a_k^{(n)}(v, w)$$

$$f_2(u, v, w) = f_1(u, v, w) + \sum_{k=1}^2 \sum_{n=0}^{q_k} \beta_k^{(n)}(v) \times \left[b_k^{(n)}(u, w) - \frac{\partial^n}{\partial v^n} f_1(u, v_k, w) \right]$$

$$f(u, v, w) = f_2(u, v, w) + \sum_{k=1}^2 \sum_{n=0}^{r_k} \gamma_k^{(n)}(w) \times \left[c_k^{(n)}(u, v) - \frac{\partial^n}{\partial w^n} f_2(u, v, w_k) \right] \tag{2}$$

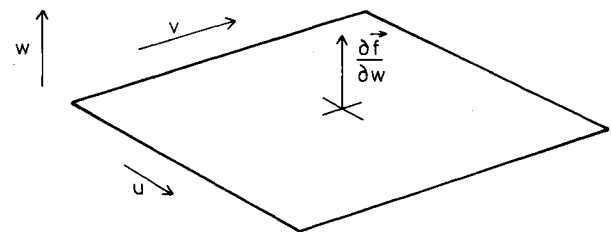


Fig. 2 Example of an out-of-surface derivative of f .

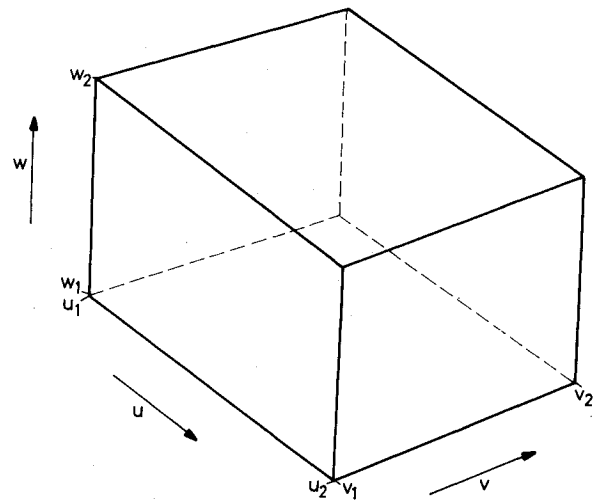


Fig. 3 The parametric domain with $f(u, v, w)$ and a finite number of out-of-surface derivatives of f specified on the six boundaries.

The function f now defines a transformation from the region $u_1 \leq u \leq u_2, v_1 \leq v \leq v_2, w_1 \leq w \leq w_2$ in u, v, w space to some arbitrarily shaped region of x, y, z space. As in the previous case, it is possible to show that the result is independent of the specific ordering of the successive univariate interpolation directions if the specified data is consistent, i.e., if certain continuity conditions are satisfied at the intersections of the six surfaces of the parametric box.

The generalized transfinite interpolation method described thus offers the possibility of generating complex global three-dimensional transformations with geometry data specified only on the outer boundary of the parametric domain. A natural question is whether anything has been gained by this alternative method, since the specification of interior surfaces has just been replaced by the specification of derivatives at the boundary. The answer is yes, because it turns out that the specification of out-of-surface derivatives is a much simpler task, as will be evident from the application of the method. In fact, the derivatives can be generated by rather simple analytic expressions and controlled by a small number of parameters, thus greatly reducing the amount of necessary geometry data.

Generally speaking, the method of transfinite interpolation, generalized in the sense described, is a very simple and straightforward concept that offers virtually unlimited possibilities; but for any particular application, it is necessary to supply a certain amount of geometry data to obtain a certain degree of control of the transformation. It is up to the user to balance the requirements of minimum input geometry data and maximum control. For the applications described in this work, it is believed that a reasonable compromise has been obtained.

Transformations, Discretizations, and Grids

The purpose of generating a global transformation that maps the physical domain as defined in the Cartesian x, y, z space to a box-like region in u, v, w space is to obtain a discretization of the physical domain that conforms to the boundaries of the problem and is in some sense smooth. This is accomplished by uniformly discretizing the slab in u, v, w space and then using the global transformation to find the corresponding grid points in x, y, z space. The word "grid" is generally used as a label for a complete set of grid points, but because of the close relationship between the grid points in x, y, z space and the underlying transformation, it is sometimes used as a label for the transformation itself.

The purpose of generating a smooth grid that conforms to the physical boundaries of the problem is, of course, to solve the partial differential equations specified in the problem by some numerical integration scheme, capable of handling general nonorthogonal curvilinear coordinates. There exists a large variety of such numerical methods and each method puts certain demands on the grid and, therefore, also on the grid generation procedure. Pure finite-difference methods are grid point oriented and require not only the grid points but also the metrics of the transformation at the grid points whereas finite-volume methods and finite-element methods are cell oriented and require only grid points. Depending on the actual mathematical model used, there are also different requirements on mapping characteristics and branch cuts. Whatever the requirements are, the generalized transfinite interpolation method is capable of satisfying them, since it can give any number of partial derivatives of the mapping function (provided that the specified boundaries are sufficiently smooth) and also handle a wide variety of different types of mappings.

Perhaps the greatest problem of grid generation is not how to construct grids, for in the transfinite interpolation concept we have a basic tool of great generality. Rather, the problem is defining in sufficient detail what qualities and properties in a grid are desirable for a particular numerical model. Existing knowledge is fundamentally empirical and it is felt that additional knowledge must be learned in a cut-and-try fashion.

Mapping Type

Before discussing the details of the application of the generalized transfinite interpolation method to the generation of three-dimensional grids around wing-body configurations, it is useful to consider some different mapping types that can be used in this specific case and to compare these in terms of computational efficiency. The term "mapping type" is here used in a very loose sense and should be interpreted as meaning the "basic characteristics of the transformation between the parametric box and the physical domain." This should be clarified by Fig. 4, where some different mappings are shown. The basic grid types given here are not, of course, the only possible types for a wing geometry, but they are the most natural ones in terms of geometry specification, since wings usually are defined by chordwise sections. The designations given in the figure are the accepted standard symbols for two-dimensional grid types and the natural generalization to three dimensions is to give two symbols, one to characterize the chordwise type and the other to characterize the spanwise type.

In the case of flow around a wing alone, it is clear that grid type O-O offers the most efficiency in terms of computational work for a given resolution, since it gives the greatest density of grid points around the wing for a given total number of grid points. For a wing-body configuration, however, it is not that simple. If the body is viewed as a simplified fluid displacing object and if the influence of the body on the wing is the main point of interest, then it is clear that grid type O-O is still the most efficient. If, on the other hand, the details of the flow around the entire body are just as important as the details of the wing flow, it is possible that some other grid type is better suited for the task. In this work, the emphasis has been on the wing flow and therefore the density of grid points around the wing has been used as a criterion for judging the different grid types. Using grid type O-O as a standard, it is possible to calculate, for each alternative grid type, the equivalent number of grid points that give a comparable resolution in the vicinity of the wing. The result of such a comparison is shown in Fig. 5. It must be stressed that this comparison depends on a number of factors and therefore is not exact in an absolute sense, but it does give an

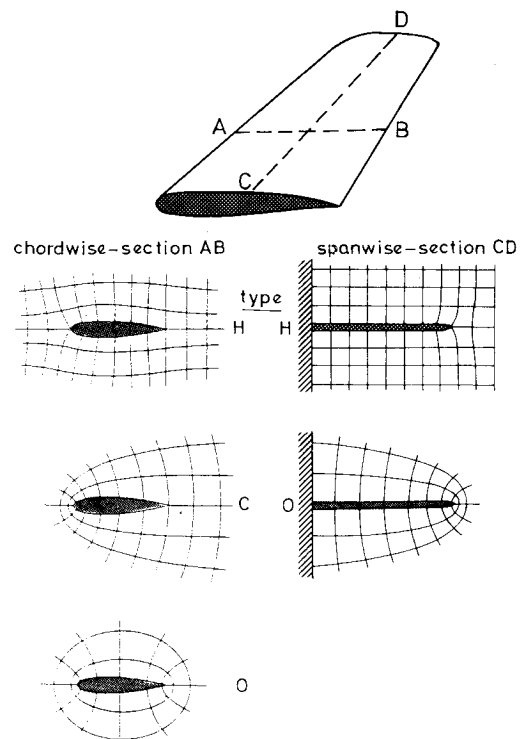


Fig. 4 Basic mapping types for a wing.

indication of the relative efficiency of each grid type. As can be seen from the comparison, grid types O-O and C-O seem to be the two "best" types. Since both mappings are of type O in the spanwise direction, they have the additional advantage of offering an improved resolution of the flow around the wing tip.

The basic mapping characteristics of the O-O grid type are shown in Fig. 6. In this case, the entire wing surface is mapped to the "bottom" surface of the parametric box (the $w = w_1$ plane), the outer spherical boundary is mapped to the "top" surface ($w = w_2$), and the plane-of-symmetry + body (the body is seen as a distortion of the plane-of-symmetry) is mapped to one of the "side" surfaces ($v = v_1$). Thus, there are three surfaces where the mapping function f must be specified. In addition, derivatives of f with respect to the w parameter must

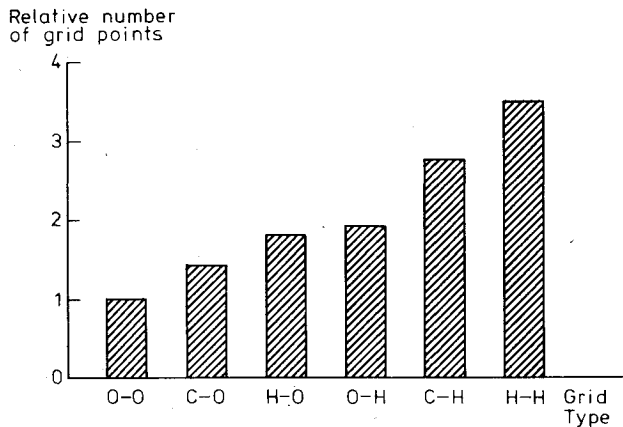


Fig. 5 Comparison of alternative grid types in terms of relative number of grid points for approximately equal resolution.

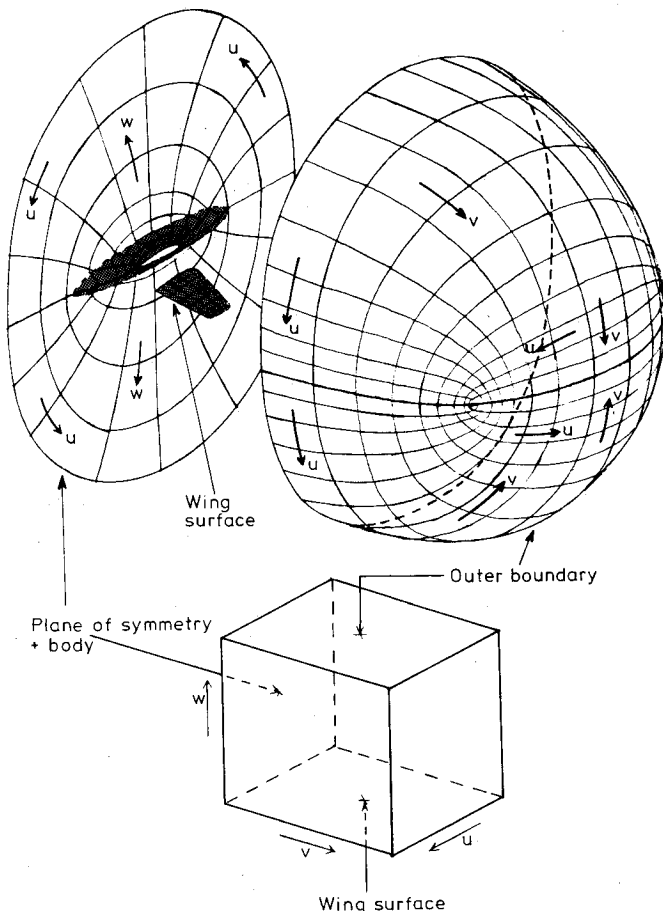


Fig. 6 Mapping characteristics of grid type O-O.

be specified on the $w = w_1$ plane (corresponding to the wing surface), thereby providing the out-of-surface derivatives needed by the generalized transfinite interpolation method to control the transformation near the wing. The details of this will be treated in a following section.

A characteristic feature of the O-O grid type is that parts of the outer boundary of the parametric box constitute branch cuts, i.e., the corresponding surfaces in the physical domain are "folded" into the interior of the domain. At these branch cuts, a point in x, y, z space is represented by two points in u, v, w space. This means that for any flow calculation, it is necessary to find appropriate continuity conditions at the branch cuts. In this case, the planes $u = u_1$ and $u = u_2$ constitute one branch cut and the plane $v = v_2$ is turned into another one.

A characteristic feature of all mapping types is the existence of singularities in the mapping function. This will be discussed in the following section.

Singularities

A fundamental difference between transformations in two dimensions ($R^2 \rightarrow R^2$) and three dimensions ($R^3 \rightarrow R^3$) is the fact that in the latter case, it is impossible to define a single smooth transformation that maps the region outside any closed smooth body (topologically equivalent to a sphere) to a box-like region like the parametric box previously mentioned, without introducing mapping singularities. This can be demonstrated just by looking at the subproblem of mapping the surface of the closed body to a rectangular area, which is illustrated in Fig. 7. Starting with the rectangular area in the parametric space, the first step in the transformation to a three-dimensional closed body is to "roll" the rectangle into a cylinder. From here there are two fundamentally different paths to follow. One path is to shrink the "holes" of the cylinder into points thereby creating two singular points of polar type. The other path is to shrink the holes of the cylinder into lines thereby creating four singular points of parabolic type. There are, of course, other paths to follow that create more complex singularities, but the polar and parabolic

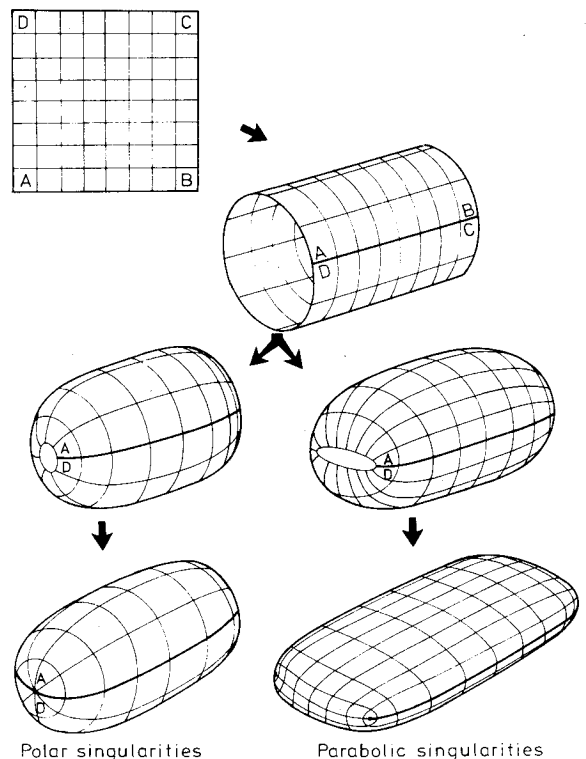


Fig. 7 Two basic types of transformations $R^2 \rightarrow R^3$ for a closed smooth body topologically equivalent to a sphere.

singularities are the two simplest types. As is indicated in Fig. 7, the parabolic type of singularity appears to be nicely suited for a wing-like geometry whereas the polar type is better suited for a blunt body.

Going back to the original problem of mapping the three-dimensional region outside the closed body to a box-like region, it is clear that one way of accomplishing this is to introduce an outer boundary in the form of a larger closed surface and then defining a third coordinate family in the outward direction, starting at the inner body surface and ending at the outer boundary. This would turn the singular points on the body surface into singular lines, stretching between the inner and outer surfaces. A necessary condition is, naturally, that both surfaces have similar surface transformations, with the same set of singular points. Figures 8 and 9 illustrate this for the two different singularity types. It should be noted that Fig. 9 also shows the essential character of the singularities in the O-O type of grid previously described, in which case there are two parabolic singular lines (actually four, with symmetry taken into account), one emanating from the leading edge of the tip and the other from the trailing edge of the tip of the wing.

A further analysis of possible transformations for the exterior-region problem shows that there are two distinct classes of mappings of which one includes all mappings with singular lines emanating from the body surface but not lying on the body surface, and the other includes all mappings with at least one singular line actually lying on the body surface. For a closed body with a salient edge, like a wing surface, the situation is complicated by the fact that in this case there is a singular line along this edge for all conceivable mappings. This indicates that it is necessary to make a distinction between curvature induced singularities, which are real singularities in a physical sense, and artificial singularities, which are caused by the mapping only.

Even though the existence of artificial singular lines in the transformation for the exterior region problem can cause some numerical difficulties, numerical results indicate that as long as the singular lines do not interfere too much with the boundary conditions of the body surface (especially at some critical points), the adverse effects are limited to the neighborhood of the singularities. This should favor the class of transformations that do not have artificial singular lines lying on the body surface, for example the O-O type of grid.

Grid Generation Procedure

The grid generation procedure for the O-O type of grid is summarized in the following points: 1) definition of the wing surface (corresponding to the $w=w_1$ surface of the parametric box); 2) generation of out-of-surface derivatives on the wing surface; 3) definition of the outer boundary (corresponding to the $w=w_2$ surface of the parametric box); 4) definition of blending functions for interpolation in the w direction (between wing surface and outer boundary); 5) interpolation in the w direction (first step of the generalized transfinite interpolation procedure); 6) definition of the combined plane-of-symmetry and body surface (corresponding to the $v=v_1$ surface of the parametric box); 7) definition of blending functions for interpolation in the v direction; and 8) interpolation in the v direction (second, and in this case final step of the generalized transfinite interpolation procedure).

The purpose of this section is not to give all the fine details of these procedure steps, but rather to demonstrate the applicability of the generalized transfinite interpolation concept and to give an idea of the possibilities it offers for other applications.

In the first step, definition of the wing surface, we need a parametric representation of the wing surface in the form $x=x(u',v')$, $y=y(u',v')$, $z=z(u',v')$ where the local parameters u' and v' are related to the global mapping

parameters u and v by some stretching functions, $u'=f(u)$, $v'=g(v)$.

When these five functions are specified, it is possible to map the wing surface to the bottom surface ($w=w_1$) of the parametric box

$$f(u,v,w_1) = [x(f(u),g(v)), y(f(u),g(v)), z(f(u),g(v))]$$

As shown in a previous section, the O-O type of grid assumes that the u parameter varies only in the chordwise direction on the wing (around each wing section) and that the v parameter varies only in the spanwise direction (between the wing sections), and except for the stretching, the local parameters u' and v' must be similar. As an example of a typical set of parameters we give the following.

$$u' = \pm\sqrt{x/c} \quad ; \quad 0 \leq x/c \leq 1$$

$$v' = 1 - \sqrt{1 - 2y/b}; \quad 0 \leq 2y/b \leq 1$$

where x/c is the relative chord position and $2y/b$ is the relative span position on the wing. The sign of u' is defined to be

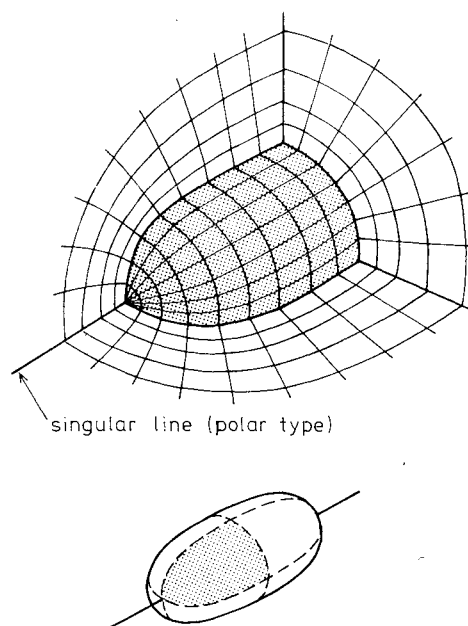


Fig. 8 Three-dimensional grid with a singular line of polar type.

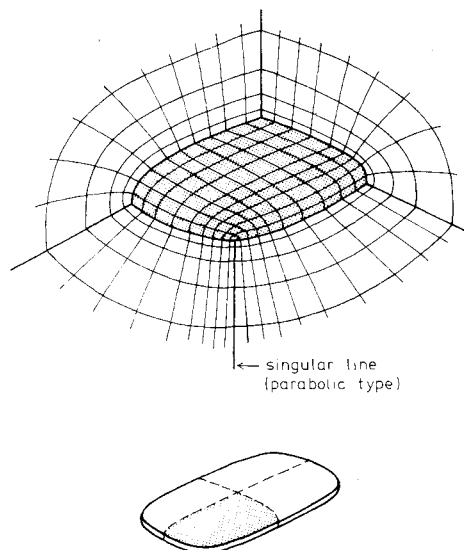


Fig. 9 Three-dimensional grid with a singular line of parabolic type.

positive on the upper side of the wing and negative on the lower side. With these parameters, it is possible to define the wing surface either in analytic form or by interpolating between available wing coordinates. The purpose of the stretching functions f and g is to control the distribution of grid points on the wing surface independently of the actual surface definition.

The second step, generation of out-of-surface derivatives on the wing surface, is accomplished by copying the behavior of two-dimensional orthogonal transformations locally. This is best described by first looking at a simple two-dimensional case like an ellipse in a Cartesian coordinate system as shown in Fig. 10. To generate derivatives of the coordinates x and y with respect to the outgoing parameter w for this case, it is natural to analyze the classical elliptic coordinate system in this respect. A simple analysis gives the result that the derivatives of x and y with respect to w at the surface of the ellipse can be written as follows:

$$\begin{aligned} \frac{\partial x}{\partial w} &= kex & \frac{\partial y}{\partial w} &= \pm k\sqrt{a^2 - x^2} \\ \frac{\partial^2 x}{\partial w^2} &= k^2x & \frac{\partial^2 y}{\partial w^2} &= \pm k^2e\sqrt{a^2 - x^2} \\ \frac{\partial^3 x}{\partial w^3} &= k^3ex & \frac{\partial^3 y}{\partial w^3} &= \pm k^3\sqrt{a^2 - x^2} \\ \frac{\partial^4 x}{\partial w^4} &= k^4x & \frac{\partial^4 y}{\partial w^4} &= \pm k^4e\sqrt{a^2 - x^2} \end{aligned}$$

etc.

The factor k is here a simple scaling factor that determines the concentration of grid points in the w direction. To apply these results to a two-dimensional wing section, it is necessary to use them locally, i.e., the ellipse constants a and e must be replaced by effective local constants at the leading and trailing edge of the section. For a fully three-dimensional wing geometry, it is also necessary to incorporate the wing tip, which means that the procedure must be extended to handle the spanwise variation also. The details of this will not be discussed but it is a relatively simple and straightforward procedure.

The end result of these manipulations is a set of relatively simple expressions giving the out-of-surface derivatives of the mapping function f as functions of the wing geometry only and controlled by a small number of user-defined constants. As an example of the degree of control that this method offers, Fig. 11 shows details of different grids generated at the trailing edge of a wing section. It is clear that the possibilities of local control by directly controlling the derivatives of the mapping function f are virtually without limit.

The third step, definition of the outer boundary, is accomplished by defining a parametric representation of the

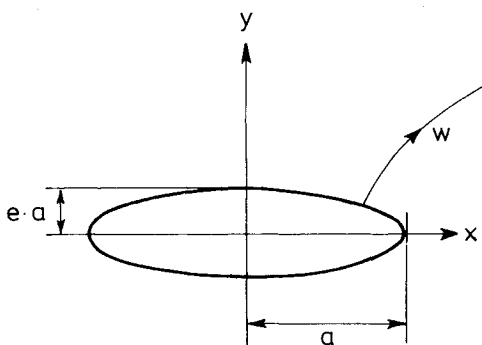


Fig. 10 Simplified geometry for generation of out-of-surface derivatives.

boundary surface in terms of the global mapping parameters u and v

$$x=x(u,v), y=y(u,v), z=z(u,v)$$

and then mapping this surface to the top surface ($w = w_2$) of the parametric box. The definition of the parametric representation of the boundary surface can be done either analytically or by interpolation. In this work, a two-variable version of the generalized transfinite interpolation method has been used to accomplish this. The O-O type of grid assumes that the surface grid on the outer boundary is of the same type as the inner surface grid, i.e., there must be two singular points of parabolic type.

In the fourth step, a suitable set of blending functions for interpolation in the w direction must be defined. Since these functions of w only have to satisfy certain conditions at the two boundary points w_1 and w_2 , there is an infinite number of possible functions. To give an idea of the practical aspects of this, we assume first that only first derivatives of the mapping function f are specified at the inner boundary $w = w_1$ and to simplify the analysis further we assume that $w_1 = 0$ and $w_2 = 1$. The first step of the generalized transfinite interpolation procedure according to Eqs. (2) with w chosen as the first interpolation direction, is then written

$$\begin{aligned} f_1(u,v,w) &= \gamma_1^{(0)}(w)f(u,v,0) + \gamma_1^{(1)}(w) \frac{\partial f}{\partial w}(u,v,0) \\ &+ \gamma_2^{(0)}(w)f(u,v,1) \end{aligned}$$

where f_1 is an intermediate mapping function. The blending functions $\gamma_1^{(0)}, \gamma_1^{(1)}, \gamma_2^{(0)}$, must satisfy the conditions

$$\begin{aligned} \gamma_1^{(0)}(0) &= 1 & \gamma_1^{(1)}(0) &= 0 & \gamma_2^{(0)}(0) &= 0 \\ \frac{\partial \gamma_1^{(0)}}{\partial w}(0) &= 0 & \frac{\partial \gamma_1^{(1)}}{\partial w}(0) &= 1 & \frac{\partial \gamma_2^{(0)}}{\partial w}(0) &= 0 \\ \gamma_1^{(0)}(1) &= 0 & \gamma_1^{(1)}(1) &= 0 & \gamma_2^{(0)}(1) &= 1 \end{aligned}$$

but otherwise we are free to choose any type of functions. In this particular case, a useful set of functions are the following:

$$\begin{aligned} \gamma_1^{(0)}(w) &= 1 - \frac{e^{\alpha w} - 1 - \alpha w}{e^\alpha - 1 - \alpha} & \gamma_1^{(1)}(w) &= w - \frac{e^{\alpha w} - 1 - \alpha w}{e^\alpha - 1 - \alpha} \\ \gamma_2^{(0)}(w) &= \frac{e^{\alpha w} - 1 - \alpha w}{e^\alpha - 1 - \alpha} \end{aligned}$$

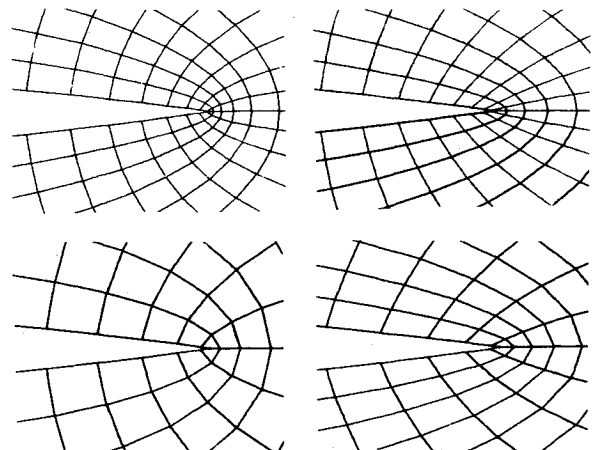


Fig. 11 Example of grid control at trailing edge of wing.

The constant α is here used to control the rate of stretching of the grid between the inner and outer surfaces. It is evident that increasing the value of α has the effect of increasing the region where the specifications on the inner boundary control the mapping function and also of increasing the rate of stretching near the outer boundary.

In the case of more than one derivative of f being specified at $w = w_j$, it is easy to define similar blending functions with the same degree of control as shown for the simplified case.

The fifth step, interpolation in the w direction, constitutes the first step of the generalized transfinite interpolation procedure according to Eqs. (2), with w as the first interpolation direction. Using the blending functions defined in the previous step, the result of the interpolation is an intermediate mapping function f_j , which conforms to the wing

geometry but not to the combined plane-of-symmetry and body surface.

In the last three steps of the total grid generation procedure, the combined plane-of-symmetry and body surface is defined and mapped to the side surface $v = v_j$ of the parametric box, a set of appropriate blending functions for interpolating in the v direction are defined, and, finally, the complete mapping function f is determined by interpolating in the v direction according to Eqs. (2). In this second interpolation step the intermediate mapping function f_j is altered so as to conform to the plane-of-symmetry and body surface combination. There is no third interpolation step in the u direction in this case since there is no data specified on the $u = u_1$ or $u = u_2$ surfaces of the parametric box.

In the preceding description of the grid generation procedure, many details have been omitted, partly because a complete description would become excessively long and partly because some of these details are still in a rather preliminary stage and undergoing a continuous development. However, the general principles of the procedure hopefully have been made clear.

Grid Examples

To illustrate the capabilities of the present grid generation method, two different grids are shown in Figs. 12 and 13 in the form of computer-plotted "views" of certain grid surfaces. The case shown in Fig. 12 is an O-O type grid for the ONERA M6 wing (a swept tapered wing) without any body and consisting of $65 \times 21 \times 15$ points in the $u, v,$ and w directions, respectively. In Fig. 12a, it is possible to see the behaviour of the constant- v grid surfaces as they span the region between the plane-of-symmetry and the branch cut outside the wing tip. The two parabolic singular lines are indicated in the figure. Also shown is a detail of the surface grid at the wing tip which indicates that the resolution obtained is quite good. Figure 12b, shows that it is possible, with the present method, to obtain a grid that gives a good resolution of both the leading-edge region and the tip region of the wing. The case presented in Fig. 13 is an O-O type grid for the RAE " W_A/B_2 " wing-body configuration and has the grid dimensions $65 \times 11 \times 25$ in the respective parameters $u, v,$

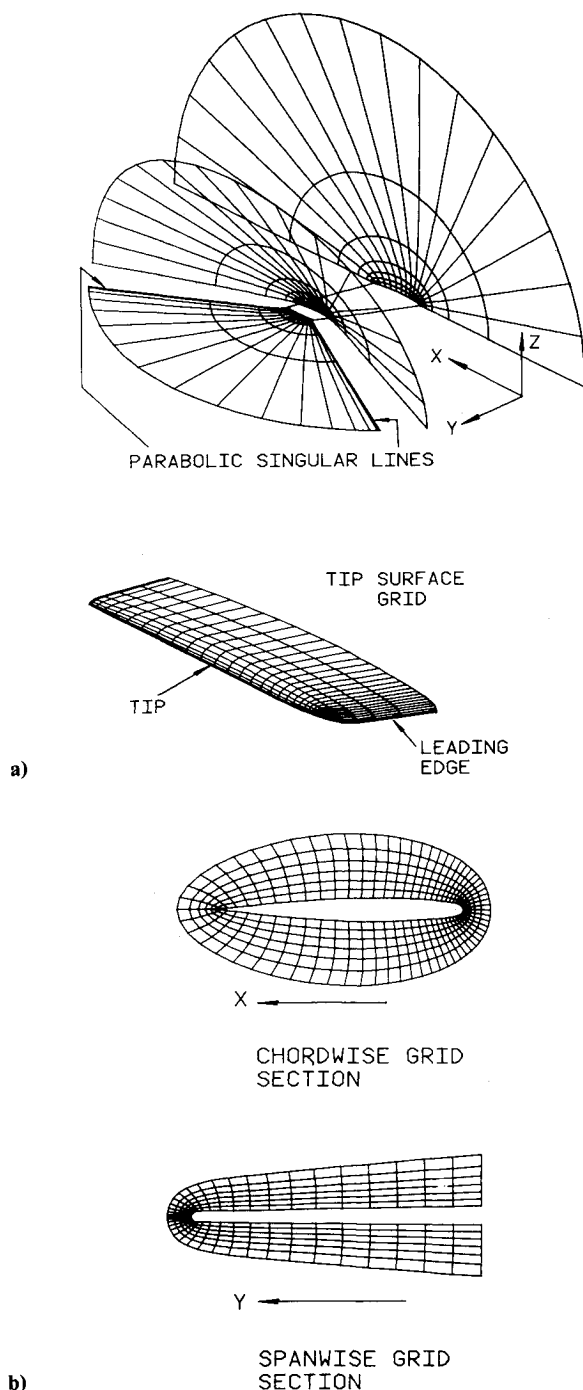


Fig. 12 a) Oblique view of the upper half of an O-O type grid for the ONERA M6 wing. The surface grid at the wing tip is shown enlarged. b) Planar view of chordwise and spanwise grid surfaces.

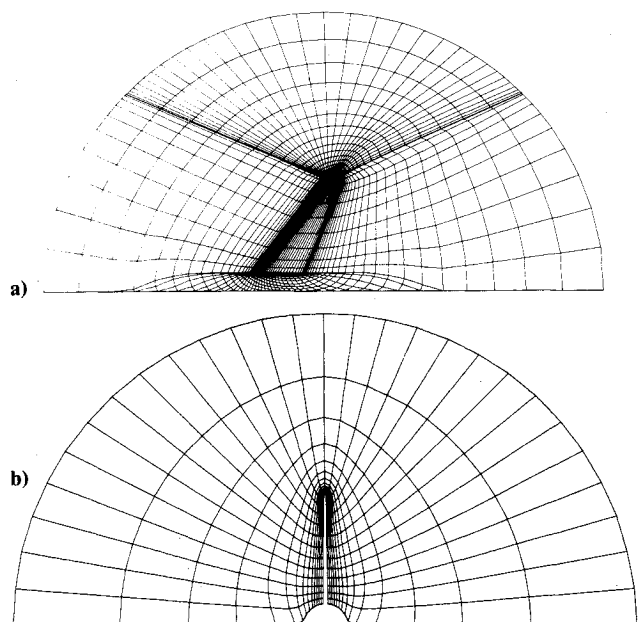


Fig. 13 a) Planar view of the upper half of an O-O type grid for the RAE W_A/B_2 wing-body configuration. Grid dimensions: $65 \times 11 \times 25$. b) Planar view of a spanwise grid surface showing the cross section of the wing and fuselage.

w. Figure 13a, which gives a planar view of selected surfaces of this grid as seen from above, shows that although the grid conforms to the body surface, it is not aligned with the line separating the body from the plane-of-symmetry, since the body is only seen as a distortion of the plane-of-symmetry. This is clearly seen in Fig. 13b, which gives another view of a constant- u grid surface.

Corresponding grid plots of C-O type grids have already been given in Ref. 2 and therefore none of these are shown here.

Concluding Remarks

This paper presents a very general method for mesh construction by transfinite interpolation and it is emphasized that there is at present a lack of theory to guide us in the development of all the many small details that go into the generation of a grid. Two areas stand out for future theoretical study. The full understanding and analysis of the way mesh singularities affect the solution procedure and a

quantitative basis for the evaluation of the quality of a given mesh.

The computer program of this mesh generation method is available for public use through the CDC Cybernet Cyber 205 Software Services.

References

¹Gordon, W. J. and Hall, C. A., "Construction of Curvilinear Coordinate Systems and Applications of Mesh Generation," *International Journal of Numerical Methods in Engineering*, Vol. 7, 1973, pp. 461-477.

²Eriksson, L. E., "Three-Dimensional Spline-Generated Coordinate Transformations for Grid around Wing-Body Configurations," *Numerical Grid Generation Techniques*, NASA CP 2166, 1980.

³Rizzi, A. W., "Damped Euler-Equation Method to Compute Transonic Flow Around Wing-Body Combinations," *AIAA Journal*, 1982, to be published.

From the AIAA Progress in Astronautics and Aeronautics Series . . .

GASDYNAMICS OF DETONATIONS AND EXPLOSIONS—v. 75 and COMBUSTION IN REACTIVE SYSTEMS—v. 76

*Edited by J. Ray Bowen, University of Wisconsin,
N. Manson, Université de Poitiers,
A. K. Oppenheim, University of California,
and R. I. Soloukhin, BSSR Academy of Sciences*

The papers in Volumes 75 and 76 of this Series comprise, on a selective basis, the revised and edited manuscripts of the presentations made at the 7th International Colloquium on Gasdynamics of Explosions and Reactive Systems, held in Göttingen, Germany, in August 1979. In the general field of combustion and flames, the phenomena of explosions and detonations involve some of the most complex processes ever to challenge the combustion scientist or gasdynamicist, simply for the reason that *both* gasdynamics and chemical reaction kinetics occur in an interactive manner in a very short time.

It has been only in the past two decades or so that research in the field of explosion phenomena has made substantial progress, largely due to advances in fast-response solid-state instrumentation for diagnostic experimentation and high-capacity electronic digital computers for carrying out complex theoretical studies. As the pace of such explosion research quickened, it became evident to research scientists on a broad international scale that it would be desirable to hold a regular series of international conferences devoted specifically to this aspect of combustion science (which might equally be called a special aspect of fluid-mechanical science). As the series continued to develop over the years, the topics included such special phenomena as liquid- and solid-phase explosions, initiation and ignition, nonequilibrium processes, turbulence effects, propagation of explosive waves, the detailed gasdynamic structure of detonation waves, and so on. These topics, as well as others, are included in the present two volumes. Volume 75, *Gasdynamics of Detonations and Explosions*, covers wall and confinement effects, liquid- and solid-phase phenomena, and cellular structure of detonations; Volume 76, *Combustion in Reactive Systems*, covers nonequilibrium processes, ignition, turbulence, propagation phenomena, and detailed kinetic modeling. The two volumes are recommended to the attention not only of combustion scientists in general but also to those concerned with the evolving interdisciplinary field of reactive gasdynamics.

*Volume 75—468 pp., 6×9, illus., \$30.00 Mem., \$45.00 List
Volume 76—688 pp., 6×9, illus., \$30.00 Mem., \$45.00 List
Set—\$60.00 Mem., \$75.00 List*

TO ORDER WRITE: Publications Dept., AIAA, 1290 Avenue of the Americas, New York, N. Y. 10104